MoS2 radio: detecting radio-waves with a two-dimensional (2D) transition metal dichalcogenide semiconductor

To cite this article before publication: Mircea L Dragoman *et al* 2019 *Nanotechnology* in press https://doi.org/10.1088/1361-6528/ab5123

MoS_2 radio: detecting radio-waves with a two-dimensional (2D) transition metal dichalcogenide semiconductor

Mircea Dragoman[1*], Martino Aldrigo[1], James Connolly[2], Ian M. Povey[2], Sergiu Iordanescu[1], Adrian Dinescu[1], Dan Vasilache[1], Mircea Modreanu[2]

[1]National Institute for Research and Development in Microtechnologies (IMT Bucharest), Erou Iancu Nicolae Street 126A, 077190 Voluntari (Ilfov), Romania

[2]Tyndall National Institute-University College Cork, Lee Maltings Complex, Dyke Parade, Cork, Ireland

Abstract

In this paper, we have designed, fabricated and tested a microwave circuit based on a MoS_2 self-switching diode. The MoS_2 thin film (10-monolayers nominal thickness) was grown on a 4-inch Al_2O_3/high-resistivity silicon wafer by Chemical Vapor Deposition process. The Raman measurements confirm the high quality of the MoS_2 over the whole area of the 4-inch wafer. We show experimentally that a microwave circuit based on a few-layers MoS_2 self-switching diode fabricated at the wafer level is able to detect the audio spectrum from amplitude-modulated microwave signals in the band 0.9-10 GHz, i.e. in the frequency range mostly used by current wireless communications. In particular, the 900 MHz band is widely exploited for GSM applications, whereas the 3.6 GHz band has been identified as the primary pioneer band for 5G in the European Union.

Corresponding author: mircea.dragoman@imt.ro

1. Introduction

The MoS_2 is the most studied 2D material after graphene. In deep contrast with graphene, MoS_2 (monolayer and multilayer) is a semiconductor, while graphene is a semimetal[1]. The high frequency applications of MoS_2 are scarce due two main reasons: (i) the difficulties in the growth of MoS_2 at the wafer level and (ii) its low mobility (lower than silicon). However, the wafer level growth of MoS_2 has been successfully performed by several methods, a very recent review reporting the progress of these methods being found in [2]. Even nowadays the majority of MoS_2 devices are still fabricated on flakes which do not guarantee any reproducibility of the results. Very recently, the MoS_2 mobility has been increased at the level of silicon, i.e. about 1,000 $cm^2/V{\cdot}s$ using strain techniques such as crested substrates[3].

In high-frequency applications, MoS_2 as an atomically-thick material was used previously in studies related to microwave switches[4-5], tunable microwave circuits[6], field-effect transistors[7-8] reaching a cut-off frequency of 42 GHz[9], and energy-harvesting up to 2.4 GHz[10]. In this paper, we continue the previous work for atomically-thick MoS_2 showing that a radio-frequency (RF) circuit based on a self-switching diode carved on MoS_2 is able to detect signals from the audio spectrum and beyond up to few kHz of modulation frequency.

We note that self-switching diodes (SSDs) are geometrical diodes, i.e. doping-free diodes[11], and they are formed by carving in atomically-thick semiconductor/2D material a periodic structure formed by coupled U-shaped nanostructures (see Fig. 1). An SSD can be modeled as a side gate field-effect transistor[12] where the gates are located in-plane with the source-drain channel and parallel to it, and where drain and gates are connected

all together in a short-circuit configuration, thus forming a diode[13]. The in-plane gates are separated from the transistor by etching. Thus, the diode current dependent on $\propto V^2$ is working as a square law detector, where V is the applied voltage. Therefore, an SSD can be used as a detector from microwaves up to THz using various semiconductors, like InP/InGaAs/InP, AlGaN/GaN and InAs[14-16].

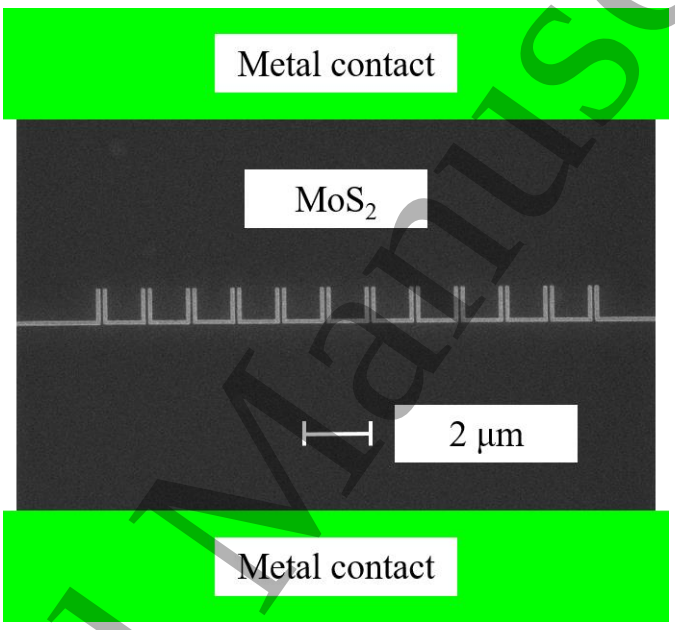

Fig. 1: SEM image of the MoS_2-based SSD.

Atomically-thick materials could directly benefit from the SSD physical principle, since no doping is required, the doping in such tiny materials being much less controllable and able to damage irreversibly the atomic lattice. In this respect, SSDs fabricated on graphene monolayers have shown very good performances[17-18]. Thus, we continue this research investigating the high-frequencies properties of SSDs based on MoS_2 at the wafer level.

2. MoS_2 growth, characterization and fabrication

The MoS_2 thin film (10-monolayers nominal thickness) was grown on a 4-inch Al_2O_3/high-resistivity silicon (HR Si) wafer by Chemical Vapor Deposition process using

a modified Applied Materials Centura ALD system at a temperature of 550°C using as precursors $Mo(CO)_6$ (99.99% purity) and 1% H_2S in Argon (99.99% purity). The Al_2O_3 thin film, with a nominal thickness of 50 nm (0.1 nm per cycle), was grown by ALD prior to the deposition of the MoS_2 thin film. ALD was performed at 250°C employing trimethylaluminium and water. Multilayers of MoS_2 were mechanically exfoliated from a commercially available natural molybdenum disulfide crystal (supplied by 2D Semiconductors) using Scotch® tape. Details of sample preparation are given elsewhere[19-20]. The exfoliated MoS_2 (≥5 layers) flakes have been used here as a reference for the Raman measurements. Raman spectra were recorded using a Renishaw Invia Reflex micro-Raman spectrometer at room temperature. The samples were excited using a CW Modu-Laser Stellar-REN laser emitting at 514.5 nm with a 0.5 mW laser power for both MoS_2 thin film and the exfoliated MoS_2 flakes. The reflecting microscope objective was 50X with a NA 0.75; the excitation spot diameter was 1 μm. The back-scattered light was dispersed by a monochromator with a spectral resolution of 1.4 cm^{-1}. The light was detected by a charge coupled device and the typical accumulation time was 20 s. Raman shifts were calibrated using an optical phonon frequency (520.5 cm^{-1}) of a silicon monocrystal reference sample.

MoS_2 belongs to the family of dichalcogenide materials, built up of weakly bonded S–Mo–S single layers. Each one of these single layers consists of two hexagonal planes of S atoms and an intercalated hexagonal plane of Mo atoms bound with the sulfur atoms in a trigonal prismatic arrangement. The symmetry space group of bulk MoS_2 is P3m1 (point group D6h). A group-theoretical analysis predicts four Raman active modes for the D6h group, i.e. three in-plane modes E_{1g}, E^1_{2g}, and E^2_{2g}, and one out-of-plane

mode A^1_g. There are four first-order Raman active modes at 32 cm^{-1} (E^2_{2g}), 286 cm^{-1} (E^1_g), 383 cm^{-1} (E^1_{2g}) and 408 cm^{-1} (A^1_g) in bulk MoS_2[19-23]. The E^2_{2g} mode arises from the vibration of an S–Mo–S layer against adjacent layers. The E^1_g mode is forbidden in back-scattering experiment on a basal plane. The in-plane E^1_{2g} mode results from opposite vibration of two S atoms with respect to the Mo atom, while the A^1_g mode is associated with the out-of-plane vibration of only S atoms in opposite directions[3-4]. The asymmetric Raman peak in MoS_2 multilayers located at around 454 cm^{-1}, is combinational band involving a longitudinal acoustic mode (*LA(M)*) and an optical mode (A_{2u}). In Fig. 2 are shown the Raman spectra of 10-layer MoS_2 deposited on Al_2O_3/HR Si substrate and for a reference 5-layers exfoliated single-crystal MoS_2. For the MoS_2 films grown on Al_2O_3/HR Si we can observe the presence of two first-order Raman active modes, at 383 cm^{-1} (E^1_{2g}) and 408 cm^{-1} (A^1_g) and the presence of the asymmetric Raman peak that is combinational band involving a longitudinal acoustic mode (*LA(M)*) and an optical mode (A_{2u})[21]. The position of the E^1_{2g} and A^1_g Raman active modes correspond to that for a 5-layer exfoliated MoS_2 confirming that our film is of high crystalline quality and that we have obtained a single phase MoS_2. The observed broadening of both E^1_{2g} and A^1_g phonon modes for the MoS_2 thin film with respect to that of the 5-layer exfoliated MoS_2 flake confirms the polycrystalline nature of our MoS_2 thin film.

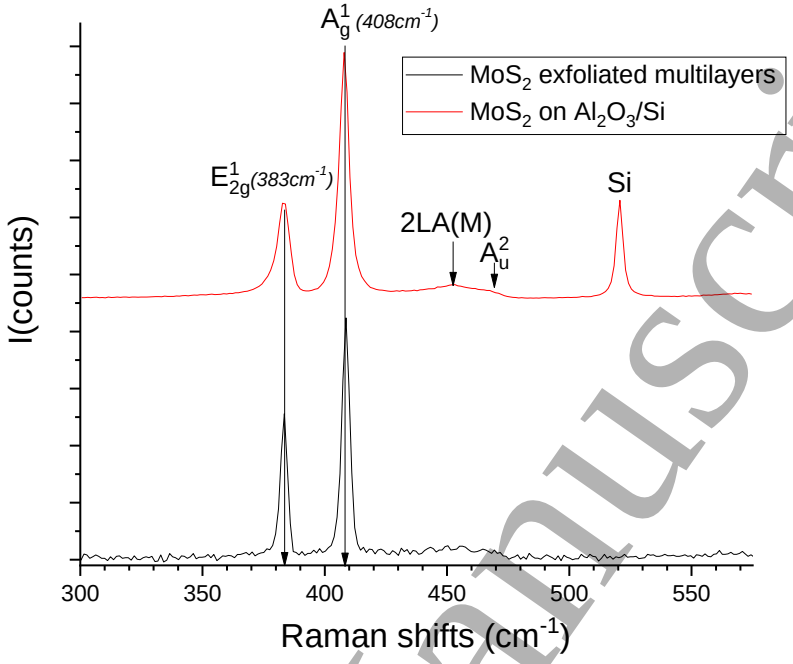

Fig. 2: Raman spectra of 10-layer MoS_2 deposited on Al_2O_3/HR Si substrate (top) and exfoliated single-crystal MoS_2 multilayer (>5 layers) (bottom). The phonon mode for the Si substrate is also observed at around 520 cm^{-1}.

We have fabricated 56 SSD diodes on MoS_2 thin film. The diodes have been patterned by e-beam lithography using PMMA 950k as electronresist and O_2 plasma etching. Then, the diodes have been covered by a negative electronresist HSQ (hydrogen silsesquioxane) patterned by e-beam lithography, defining rectangular protective areas on top of diodes and the residual MoS_2 has been etched away in O_2 plasma. The channel width of a MoS_2 SSD is 100 nm. The metallic deposition of Ti/Au (30/200 nm) has been performed in a highly directional e-beam evaporation equipment (TEMESCAL FC2000) followed by the lift-off when the sample was placed in acetone for a few hours, then sonicated in IPA.

3. DC and microwave characterization

The electrical characterization of the fabricated MoS_2 SSD-based microwave detectors has been performed using a Keithley SCS 4200 station, for which all three channels are connected with low noise amplifiers. We have measured all 56 diodes, and we have seen that 13 diodes are in shortcut due to metallization misalignments: this entailed the presence of an undesired Au layer in correspondence of diode's area, thus short-circuiting diode's anode and cathode.

The *I-V* curve of a single MoS_2 SSD diode is represented in Fig. 3a together with a fitted curve of the type $\pm\alpha V^2$ where $\alpha = 1.2$. We see that the model of a square law detector is very near to the experimental results. The measurement of 10 diodes is represented in Fig. 3b. We can see that the on/off ratio is 10^6 which points out that a MoS_2 SSD can be used in logic applications as indicated in the seminal paper of Song et al[11].

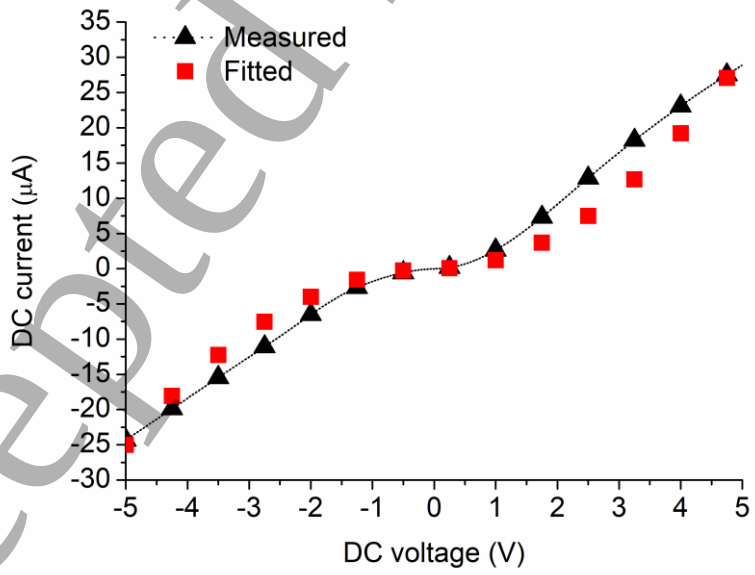

(a)

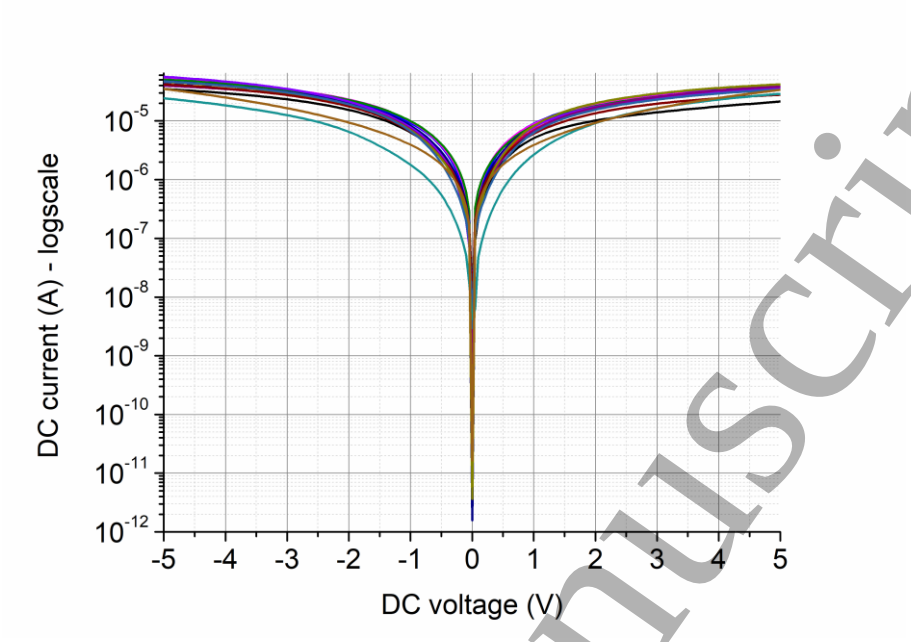

(b)

Fig. 3: (a) DC response of a single MoS_2 SSD (black dotted line with triangles: experimental results; red squares: fitted curve); (b) *I-V* curves for 10 MoS_2 SSDs.

The final circuit containing the coplanar lines (CPWs) and the tunable open stubs (thus providing different reactance values) for matching the diode to the incoming microwave signal is displayed in Fig. 4a (in the inset, the scale bar and the main dimensions are shown). In detail, the open stubs can be tuned by soldering with conductive paste one segment to the next one (hence in a selective way), in order to find the best RF matching to diode's port. For example, in the K_a band (i.e. 26.5–40 GHz) there is an improvement in RF matching to diode's port of 14 dB at 28 GHz when using the shortest stub (220 μm-long) instead of the middle-long one (620 μm-long). This solution will be extremely useful when matching the diode to an antenna (or antenna array) in a real detector (this will be the object of future research). However, for the

present case of study in which the RF source is directly connected to the diode, the effect of stub's length can be neglected, as we can estimated in a precise way the amount of power effectively delivered to the diode, even in presence of an impedance mismatch (which simply lowers the total power in input to the detector). As regards the DC pads shown in Fig. 4a, they are meant to isolate the RF signal from the DC bias line by soldering a proper decoupling capacitor, according to the operating frequency.

The microwave measurements have been performed with an experimental setup emulating a radio channel (see Fig. 4b): the CPW input port of the MoS_2 detector has been excited by a microwave generator (Agilent E8257D) with an AM modulated signal. The carrier frequency has been varied between 900 MHz and 10 GHz at various input power levels and the AM modulation signal has been chosen within the audio frequency range, with a modulation frequency up to 20 kHz. The MoS_2 SSD detectors have been placed on a probe-station and the demodulated signal has been extracted using a digital oscilloscope (Tektronix, SR560). The microwave generator has been connected via an external bias tee to a voltage source in order to provide a DC bias signal to the MoS_2 SSD. A low noise amplifier (LNA, Stanford Research SR560) has been placed at the output of the MoS_2 detector and connected to the oscilloscope in order to better visualize the detected signal and store the received data.

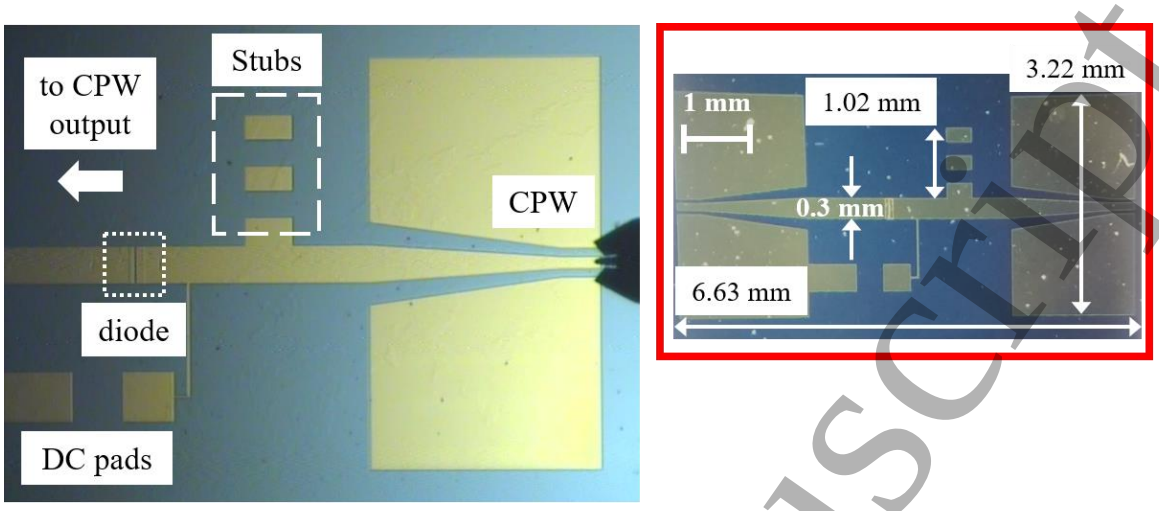

(a)

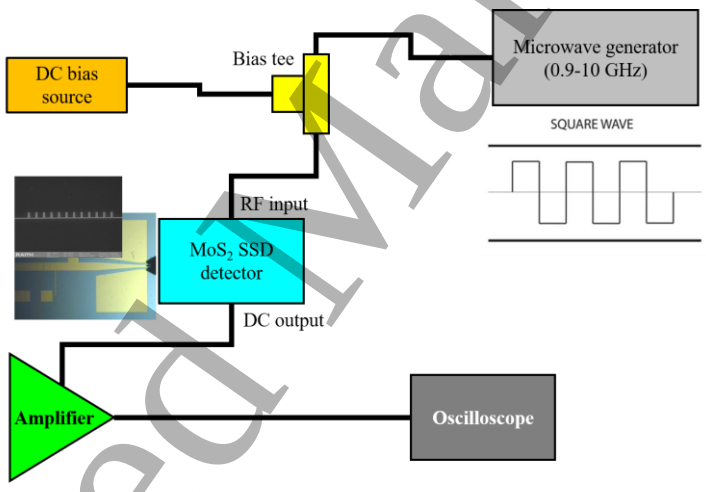

(b)

Fig. 4: (a) optical image of the MoS_2 SSD detector. Inset: scale bar and main dimensions; (b) RF/DC measurement setup schematic.

First, we have made an experiment at 0 V bias to see if the MoS_2 diode is working as a harvester, i.e. if it could transform the excited electromagnetic energy into DC voltage. In this respect, we have varied the incident power between -15 dBm up to +10 dBm for several frequencies in the range 900 MHz up to 10 GHz and the results are

presented in Figs. 5a (DC voltage) and 5b (DC power). We see that the detection at 0 V at higher and higher frequencies is possible only increasing the input microwave power. While at 900 MHz we use microwave input power in the range -15 dBm and 0 dBm which are assigned to wireless networks and Bluetooth radio, the DC response at 10 GHz requires much higher input power in the range of 5-10 dBm. We see that the DC power is in the range 0.015-35 pW depending on the frequency and on the input microwave power. Although these DC power levels are small, we can bias a microprocessor[24] used for sensing applications which consumes 35.4 pW in passive mode and 226 nW in active mode. For example, we could achieve this task by using the Bluetooth module of a mobile phone working at 900 MHz and the proposed MoS_2 SSD detector.

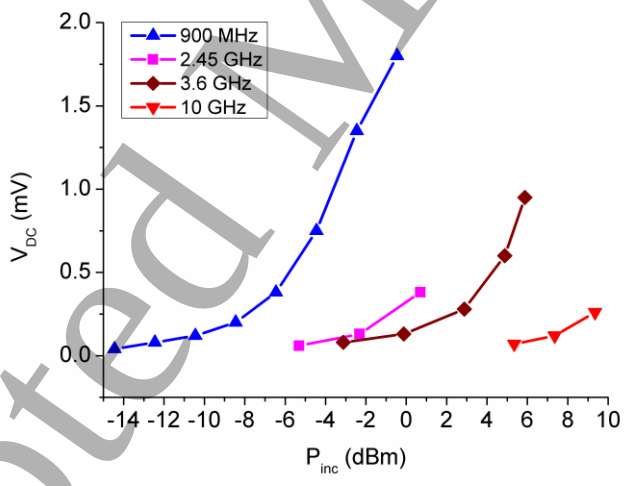

(a)

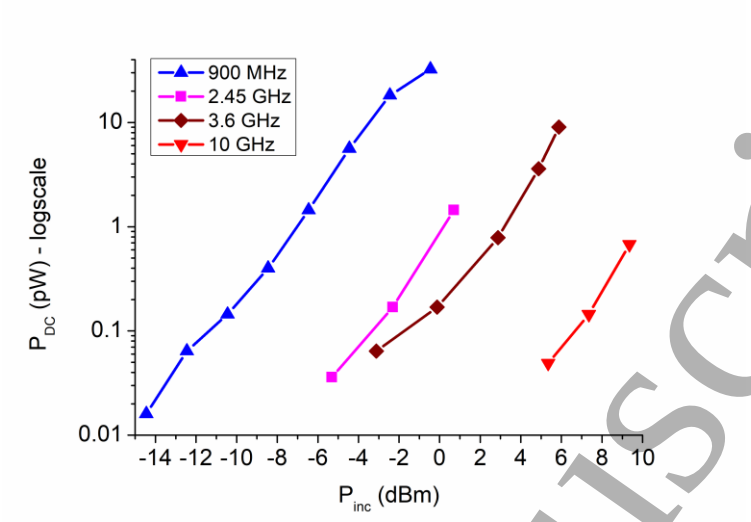

(b)

Fig. 5: Detected (a) DC voltage and (b) DC power at 0 V bias of a MoS_2 SSD excited by a microwave signal with carrier frequency of 900 MHz, 2.45 GHz, 3.6 GHz and 10 GHz.

Then, we have applied various DC biases in the range 0.1-2 V on the MoS_2 diode at two target frequencies, i.e. 900 MHz and 3.6 GHz, the detected voltages at these two frequencies being displayed in Figs. 6a and 6b (respectively), when the modulation signal frequency is 2 kHz. The responsivity at 900 MHz and 2 V bias is 100 V/W at an input power of -25 dBm, while at 3.6 GHz the responsivity is 8 V/W at an input power of -10 dBm at the same bias voltage. We have varied the audio modulation signal up to 20 KHz and we have observed that the detection signal amplitudes do not change significantly for the two carrier frequencies, the only variation being ascribed to the detected pulse durations. A detected signal with a carrier frequency of 900 MHz and 2 kHz AM modulation is represented in Fig. 7.

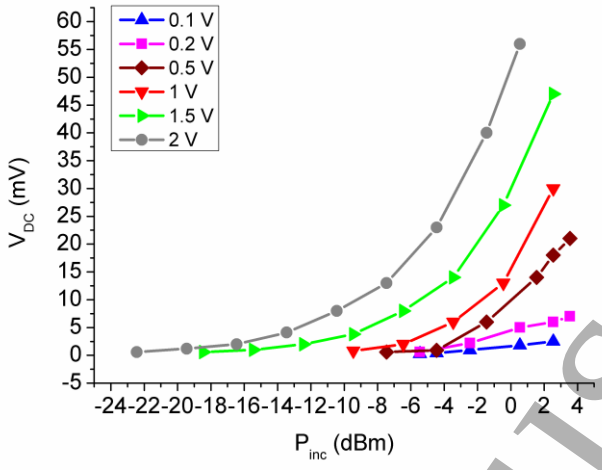

(a)

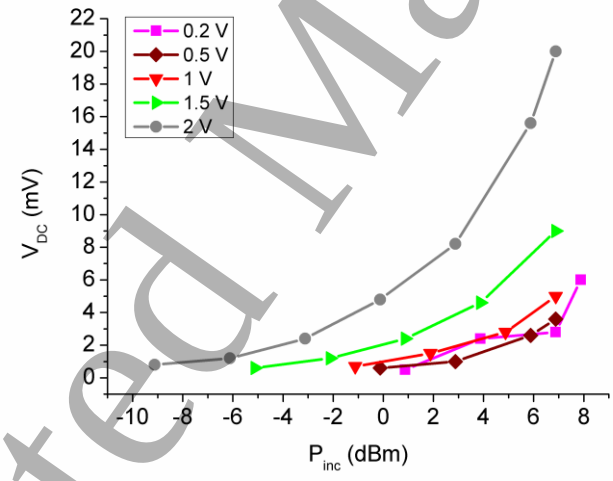

(b)

Fig. 6: Detected DC voltage of the MoS_2 SSD with a modulation frequency of 2 kHz and a carrier frequency of (a) 900 MHz and (b) 3.6 GHz, as a function of the applied voltage bias (blue line: 0.1 V bias; pink line: 0.2 V bias; brown line: 0.5 V bias; red line: 1 V bias; green line: 1.5 V bias; grey line: 2 V bias).

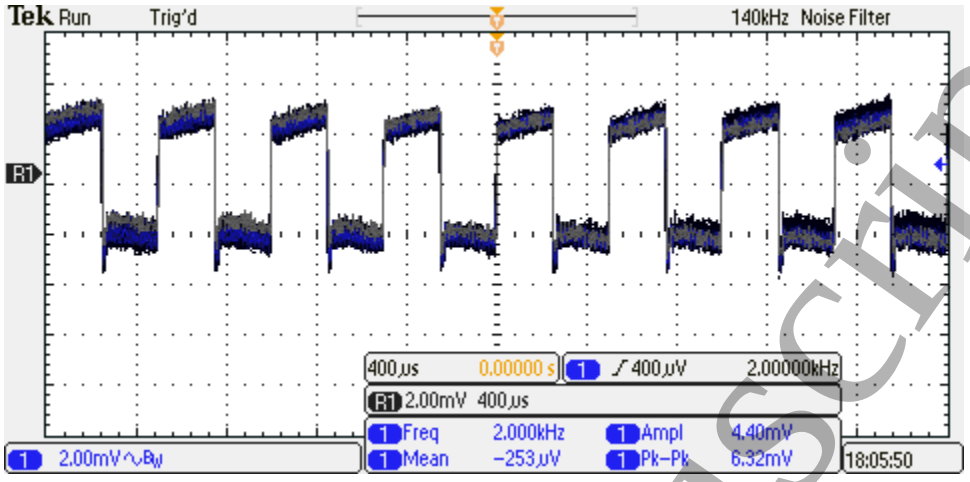

Fig. 7: time-domain detected signal at a carrier frequency of 900 MHz and 2 kHz AM modulation.

4. Conclusions

In this paper, we have designed, fabricated and tested a microwave circuit based on a MoS_2 self-switching diode. We have fabricated and tested tens of such structures on a single chip cut from an atomically-thin MoS_2/Al_2O_3/HR Si wafer. We have demonstrated that our devices are able to work also as harvesters in order to bias in a wireless mode a microprocessor, and as a radio detector within the frequency range 0.9-10 GHz, the most used band today for modern wireless communications. In particular, the 900 MHz band is widely exploited for GSM applications, whereas the 3.6 GHz band has been identified as the primary pioneer band for 5G in the European Union.

Acknowledgment. The authors acknowledge the financial support of the Romanian Ministry of Research and Innovation, CNCS-UEFISCDI, via project no. PN-III-P1-1.1-PD-2016-0535, and project no. PN-III-P4-ID-PCCF-2016-0033 “GRAPHENEFERRO”.

References

[1]M. Dragoman, and D. Dragoman, 2D Nanoelectronics Physics and Devices of Atomically Thin Materials, Springer, Heidelberg, 2017

[2]Y. Huang, and L. Liu, Recent progress in atomic layer deposition of molybdenum disulfide: a mini review, Sci China Mater 62, 913 (2019)

[3]T. Liu, S. Liu, K.-H. Tu, H. Schmidt, L. Chu, D. Xiang, J. Martin, G. Eda, C. A. Ross, and S. Garaj, Crested two-dimensional transistors, Nature Nanotechnology 14, 223 (2019)

[4]M. Dragoman, A. Cismaru, M. Aldrigo, A. Radoi, and D. Dragoman, Switching microwaves via semiconductor-isolator reversible transition in a thin-film of MoS_2, J. Appl. Phys. 118, 045710 (2015)

[5]M. Kim, R. Ge, X. Wu, X. Lan, J. Tice, J. C. Lee, and D. Akinwande, Zero-static power radio-frequency switches based on MoS_2 atomristors, Nature Communications 9, Article number: 2524 (2018)

[6]M. Dragoman, A. Cismaru, M. Aldrigo, A. Radoi, A. Dinescu, and D. Dragoman, MoS_2 thin films as electrically tunable materials for microwave applications, Appl. Phys. Lett. 107, 243109 (2015)

[7]A Sanne, R. Ghosh, A. Rai, M. N. Yogeesh, S. H. Shin, A. Sharma, K. Jarvis, L. Mathew, R. Rao, D. Akinwande, and S. Banerjee, Radio Frequency Transistors and Circuits Based on CVD MoS_2, Nano Lett. Nano Lett. 15, 5039 (2015)

[8]Y. Liu, X. Duan, Y. Huang and X. Duan, Two-dimensional transistors beyond graphene and TMDCs, Chem. Soc. Rev. 47, 6388 (2018)

[9]R. Cheng, S. Jiang, Y. Chen, Y. Liu, N. Weiss, H.-C. Cheng, H. Wu, Y. Huang, and X. Duan, Few-layer molybdenum disulfide transistors and circuits for high-speed flexible electronics, Nature Communications 5, Article number: 5143 (2014)

[10]X. Zhang, J. Grajal, X. Wang, U. Radhakrishna, Y. Zhang, J. Kong, M. S. Dresselhaus, and T. Palacios, MoS_2 Phase-junction-based Schottky diodes for RF Electronics, IEEE/MTT-S International Microwave Symposium, Philadelphia, USA, 10-15 Jun. 345 (2018)

[11]A. M. Song, et al., Unidirectional electron flow in a narrow semiconductor channel: A self-switching device, Appl. Phys. Lett. 83, 1881 (2003)

[12]B. Hähnlein, B. Händel, J. Pezoldt, H. Töpfer, R. Granzner, and F. Schwierz, Side-gate graphene field-effect transistors with high transconductance, Appl Phys Lett 101, 093504 (2012)

[13]M. Åberg, J. Saijets, A. Song and M. Prunnila, Simulation and Modeling of Self-switching devices, Physica Scripta T114, 123 (2004)

[14]C. Balocco, A. M. Song, M. Åberg, A. Forchel, T. González, J. Mateos, I. Maximov, M. Missous, A. A. Rezazadeh, J. Saijets, L. Samuelson, D. Wallin, K. Williams, L. Worschech, and H. Q. Xu, Microwave Detection at 110 GHz by Nanowires with Broken Symmetry, Nano Lett. 5, 1423 (2005)

[15]P. Sangaré, G. Ducournau, B. Grimbert, V. Brandli, M. Faucher, C. Gaquière, A. Íñiguez-de-la-Torre, I. Íñiguez-de-la-Torre, J. F. Millithaler, J. Mateos, and T. González, Experimental demonstration of direct terahertz detection at room-temperature in AlGaN/GaN asymmetric nanochannels, J. Appl. Phys. 113, 034305 (2013)

[16]A. Westlund, P. Sangaré, G. Ducournau, P.-Å. Nilsson, C. Gaquière, L. Desplanque, X. Wallart, and J. Grahn, Terahertz detection in zero-bias InAs self-switching diodes at room temperature, Appl. Phys. Lett. 103, 133504 (2013)

[17]A. Westlund, M. Winters, I. G. Ivanov, J. Hassan, P.-Å. Nilsson, E. Janzén, N. Rorsman, and J. Grahn, Graphene self-switching diodes as zero-bias microwave detectors, J. Appl. Phys. 106, 093116 (2015)

[18]M. Yasir, M. Aldrigo, M. Dragoman, A. Dinescu, M. Bozzi, S. Iordanescu, and D. Vasilache, Integration of antenna array and self-switching graphene diode for detection at 28 GHz, IEEE Electron Device Lett. 40, 628 (2019)

[19]P. Budania, P. Baine, J. Montgomery, C. McGeough, T. Cafolla, M. Modreanu, D. McNeill, N. Mitchell, G. Hughes, and P. Hurley, Long-term stability of mechanically exfoliated MoS_2 flakes, MRS Communications 7, 813 (2017)

[20]P Budania, P. T. Baine, J. H. Montgomery, D. W. McNeill, S. J. N. Mitchell, M. Modreanu, and P. K. Hurley, Effect of post-exfoliation treatments on mechanically exfoliated MoS_2, Materials Research Express 4, 025022 (2017)

[21]H. Li, Q. Zhang, C. C. R. Yap, B. K. Tay, T. H. T. Edwin, A. Olivier, D. Baillargeat, From Bulk to Monolayer MoS_2: Evolution of Raman Scattering, Advanced Functional Materials 22, 1385 (2012)

[22]P. A. Bertrand, Surface-phonon dispersion of MoS_2, Phys. Rev. B 44, 5745 (1991)

[23]A. Molina-Sánchez, and L. Wirtz, Phonons in single-layer and few-layer MoS_2 and WS_2, Phys. Rev. B 84, 155413 (2011)

[24]S. Hanson, M. Seok, Y.-S. Lin, Z.Y. Foo, D. Kim, Y. Lee, N. Liu, D. Sylvester, and David Blaauw, A Low-Voltage Processor for Sensing Applications With Picowatt Standby Mode, IEEE J. Solid State Circuits 44, 1145 (2009)